Jurnal Teknologi

Full Paper

NEW CUBIC TIMMER TRIANGULAR PATCHES WITH C^1 AND G^1 CONTINUITY

Fatin Amani Mohd Ali[a], Samsul Ariffin Abdul Karim[a,b*], Sarat Chandra Dass[a], Vaclav Skala[c], Azizan Saaban[d], Mohammad Khatim Hasan[e], Ishak Hashim[f]

[a]Fundamental and Applied Sciences Department, Universiti Teknologi PETRONAS, 32610, Seri Iskandar, Perak Darul Ridzuan, Malaysia
[b]Centre for Smart Grid Energy Research (CSMER), Institute of Autonomous System, Universiti Teknologi PETRONAS, Bandar Seri Iskandar, 32610 Seri Iskandar, Perak Darul Ridzuan, Malaysia
[c]School of Computer Science and Engineering, University of West Bohemia, Plzen
[d]School of Quantitative Sciences, UUMCAS, Universiti Utara Malaysia, Kedah, Malaysia
[e]Centre for Artificial Intelligence Technology, Faculty of Information Science and Technology, Universiti Kebangsaan Malaysia, 43600 UKM Bangi, Selangor, Malaysia
[f]Centre for Modelling & Data Science, Faculty of Science & Technology, Universiti Kebangsaan Malaysia, 43600 UKM Bangi, Selangor, Malaysia

Article history
Received
15 April 2019
Received in revised form
5 July 2019
Accepted
7 July 2019
Published online
24 October 2019

*Corresponding author
samsul_ariffin@utp.edu.my

Graphical abstract

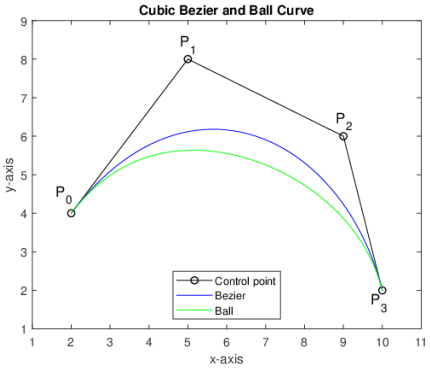

Abstract

In this study, a new cubic Timmer triangular patch is constructed by extending the univariate cubic Timmer basis functions. The best scheme that lies towards the control polygon is cubic Timmer curve and surface compared to the other methods. From the best of our knowledge, nobody has extended the univariate cubic Timmer basis to the bivariate triangular patch. The construction of the proposed cubic Timmer triangular patch is based on the main idea of the cubic Ball and cubic Bezier triangular patches construction. Some properties of the new cubic Timmer triangular patch are investigated. Furthermore, the composite cubic Timmer triangular patches with parametric continuity (C^1) and geometric continuity (G^1) are discussed. Simple error analysis between the triangular patches and one test function is provided for each continuity type. Numerical and graphical results are presented by using Mathematica and MATLAB. Results show that cubic Timmer triangular patches produces estimated result with less RMSE compared to Bèzier patches relatively by 2.01% to 7.80%. These results are significant in producing high accuracy for image and surface reconstruction.

Keywords: Cubic Timmer triangular patch, parametric continuity, geometric continuity, cubic Timmer curve, scattered

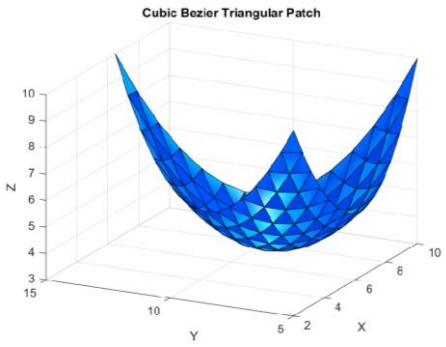

Abstrak

Dalam kajian ini, tampalan segi tiga kubik Timmer yang baru akan dibina dengan melanjutkan fungsi asas kubik univariat Timmer. Kaedah terbaik yang terletak pada poligon kawalan adalah lengkung kubik Timmer dan permukaan kubik Timmer berbanding kaedah lain. Oleh itu, tampalan segi tiga Timmer kubik baru ini dibina untuk menentukan sifat permukaan dalam bentuk segi tiga. Keselanjaran parametrik (C^1) dan keselanjaran geometri (G^1) digunakan untuk membina segi tiga kubik Timmer yang baru. Analisis ralat mudah di antara tompok segi tiga bagi setiap keselanjaran dan satu fungsi ujian disediakan. Keputusan berangka dan grafik dibentangkan menggunakan Mathematica dan MATLAB. Keputusan kajian menunjukkan tampalan segi tiga Timmer kubik menghasilkan keputusan anggaran dengan Ralat Punca Purata Kuasa dua yang secara relatif lebih rendah, iaitu 2.01% to 47.03% berbanding tampalan *Bèzier*.Keputusan ini penting dalam menghasilkan ketepatan yang tinggi untuk rekonstruksi imej dan permukaan.

Kata kunci: Tampalan segi tiga kubik Timmer, keselanjaran parametrik, keselanjaran geometri, lengkung kubik Timmer, permukaan kubik Timmer

1.0 INTRODUCTION

In 1974, R. Barnhill and R. Riesenfeld coined the term of Computer Aided Geometric Design (CAGD) at one of the conferences in the University of Utah, U.S.A. [13]. CAGD was developed to bring some of the computers' benefits to industries. Basically, the creation of surfaces and curves can be described as a mathematical representation with some geometric properties. A familiar way of modelling some geometry shape is to represent the curve or surface of an object as a patchwork of parametric polynomial pieces. This polynomial pieces can be represented as Bèzier curves and surfaces with degree n, which it is convenient for the user for making interactive designs. One of the famous methods of constructing curves and surfaces is using cubic Bèzier followed by cubic Ball. In 1980, the cubic Timmer curve was introduced by Harry Timmer. Cubic Timmer curve has one special advantage which is even though it does not all fulfil the convex hull property, the cubic Timmer curve will lie closer to the control polygon compared to cubic Bèzier and cubic Ball, and sometimes, the curve can be used to mimic the control polygons.

Some surfaces are more suitable with triangles than quadrilaterals surfaces because of the partition of the domain will be more convenient with triangular regions. Therefore, Timmer triangular patches are used to construct surfaces over arbitrary triangular meshes. A brief overview of the curve and surface construction by using quadrilaterals and triangles surfaces given in the Section 2.0.

Scattered data interpolation can be used to reconstruct the surface obtained from an experiment, for example, in the case of geological events such as rainfall distributions and geochemical compositions of a certain physical state. One of the earliest studies that addressed this problem is the paper by Shepard [20] who implemented a global scheme for scattered data. Another method is called a triangulation based scheme, i.e. the surface is reconstructed through a convex combination of Bézier triangular patches, which satisfies some degree of continuity along adjacent triangles. Research on scattered data interpolation can be found in [1-25].

Most of the previous researchers have used a cubic Bézier and a cubic Ball equation to construct curves and surfaces for both rectangular and triangular patches. Besides, the cubic basis functions constructed by Timmer [22] are only for curve and rectangular patches. At the moment, nobody has extended the Timmer methodology on rectangular patches to the cubic Timmer triangular patches. Thus in this study, the extension of the univariate cubic Timmer to the bivariate triangular basis is discussed. Hence, the construction of this new Timmer triangular patches will be compared and analyzed with the previous scheme.

Said [19] constructed the basis function called the cubic Bèzier-like with two positive parameters that are denoted as α and β. By choosing the appropriate values for α and β, the basis functions can be reduced to cubic Bèzier and Ball basis functions. Ali [1] introduced another cubic Bèzier-like basis function through a Hermite curve.

Goodman and Said [122] constructed a suitable C^1 triangular interpolant for scattered data interpolation using the convex combination scheme. The data given determine the suitable Bezier ordinates so the adjacent patches meet with the C^1 continuity requirement. Their works is different from Foley and Opitz [11], even though both developed a C^1 cubic triangular convex combination scheme. Foley and Optiz [11] proposed cubic precision boundary derivatives to construct scattered data interpolation. Chang and Said [6] further extended this approach to

C^2 quintic triangular surface scheme that requires up to the second-order partial derivatives values. Brodlie *et al*. [5] have discussed the positivity preserving by using meshfree methods that involving some optimization problem.

Said and Wirza [20] adopted the interpolant scheme proposed by Goodman and Said [11] to construct scattered data interpolation by using cubic Ball triangular patches since the cubic precision method was a bit difficult to them. The data that they are used enabled them to determine appropriate Ball triangular points such that adjacent triangular patches fulfill the C^1 continuity.

Zhu *et al*. [25] discussed a new quartic rational Said-Ball-like basis function and applied it to generate a class of C^1 continuous quartic rational Hermite Interpolations splines with local tension shape parameters. Then, they extend the basis function to a triangular domain. Saaban *et al*. [18] have constructed C^2 interpolant to preserve the positivity of rainfall data in Peninsular Malaysia. The quantic Bèzier triangular patches is used to construct the surface.

Chan and Ong [6] described the local scheme for range-restricted scattered data interpolation by using cubic triangular Bézier patches. The interpolating surface was obtained piecewise through a convex combination of three cubic Bézier triangular patches. Luo and Peng [14] described the C^1 rational spline as a piecewise rational convex combination of three cubic Bézier triangular patches that sharing the same boundary Bézier ordinates. The sufficient conditions for non-negativity were derived on the boundary Bézier ordinates of the adjacent triangle and the normal derivatives at the data sites.

Karim and Saaban [12] visualized the terrain data of central region of Malaysia by using cubic Ball triangular patches. Ramli and Ali [16] extended the Timmer method to higher order Timmer blending functions which are quartic and quantic Timmer methods. They designed of a few objects i.e. glass, sink and vase using their proposed methods. Awang *et al*. [3] reconstructed the surface of scattered data points by using six different of test functions. Their tested the effectiveness of Delaunay triangulation when the points are removed. Awang and Rahmat [3] developed a smooth surface using cubic Bèzier triangular patch with the Graphical User Interface (GUI) function to represent the results and the comparison of all the surface that generated using six different test functions.

2.0 METHODOLOGY

2.1 Bèzier-Like Cubic Basis Functions

The Bèzier-like basis functions have two free parameters to change the shape of the curve. As compared to cubic Bèzier, the way to change the shape of the curve is by adjusting the control points. By these basis functions are more convenient because the shape can be by altering the value of the free parameters. The cubic Bèzier-like basis functions containing two parameters α and β for $u \in [0,1]$ are defined as follows [13]:

$$\left.\begin{aligned} B_0^3(u) &= (1-u)^2(1+(2-\alpha)u) \\ B_1^3(u) &= \alpha(1-u)^2u \\ B_2^3(u) &= \beta u^2(1-u) \\ B_3^3(u) &= u^2(1+(2-\beta)(1-u)) \end{aligned}\right\} \quad (1)$$

The Bèzier and Ball basis functions will be obtained when $\alpha = \beta = 3$ and $\alpha = \beta = 2$ respectively. If the parameters $\alpha = \beta = 4$ then the basis functions above known as Timmer basis functions.

The parametric cubic Bèzier-like curve is defined as

$$P(u) = \sum_{i=0}^{3} p_i B_i^3(u), u \in [0,1] \quad (2)$$

where $p_i, i = 0,1,2,3$ are the control points while $B_i^3(u), i = 0,1,2,3$ are the basis functions. Figure 1 shows three different curves obtained from three different free parameters.

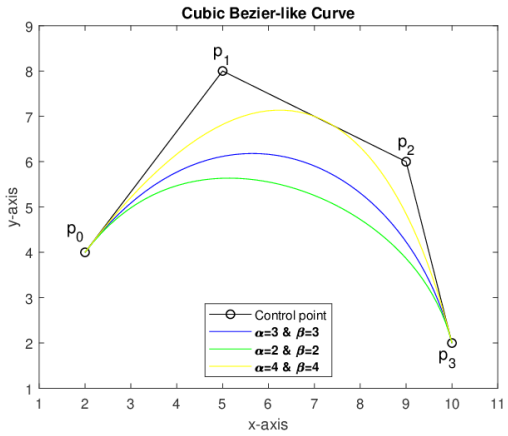

Figure 1 Cubic Bezier-like curve

Based on Figure 1, the curve for parameter $\alpha = \beta = 4$ which known as cubic Timmer curve lies towards the control polygon better than others. The concept of cubic Timmer method is proposed by Harry Timmer (1980) to produce curve and surface [22]. The cubic Timmer basis functions are defined as follows.

$$\left.\begin{aligned} T_0^3(u) &= (1-2u)(1-u)^2 \\ T_1^3(u) &= 4u(1-u)^2 \\ T_2^3(u) &= 4u^2(1-u) \\ T_3^3(u) &= (2u-1)u^2 \end{aligned}\right\} \quad (3)$$

The cubic Timmer curve is as follows:

$$T_3(u) = \sum_{i=0}^{3} a_i T_i^3(u) \quad (4)$$

where a_i denotes as the control point, while $T_i^3(u), i = 0,1,2,3$ are the cubic Timmer basis functions [19]. In Figure 2, 3 and 4 show that the bi-cubic Timmer surface and the equation consist of control points denoted as a_i and the basis functions $T_i^3(u), T_j^3(v), i = 0,1,2,3$ can be represented by:

$$T(u,v) = \sum_{i=0}^{3}\sum_{j=0}^{3} a_i T_i^3(u) T_j^3(v) \qquad (5)$$

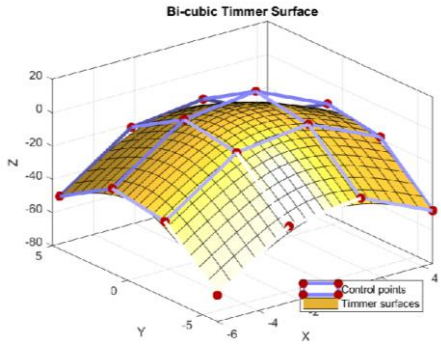

Figure 2 Bi-cubic Timmer surface

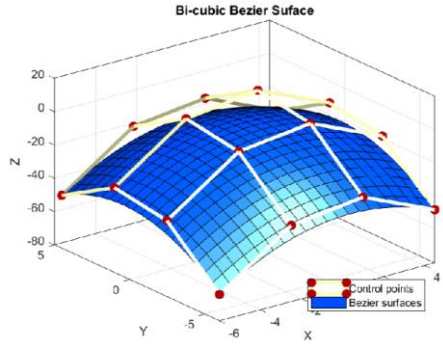

Figure 3 Bi-cubic Bèzier surface

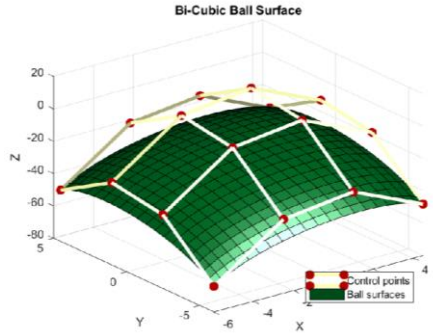

Figure 4 Bi-cubic Ball surface

Based on Figure 2 until 4, bi-cubic Timmer surface lies towards the control polygon better than bi-cubic Bèzier and Ball surface. Some applications of Timmer curve can be furthered explored. Figures 5 and 6 show the letter "f" and letter "t" which consists 25 and 20 cubic segments, respectively.

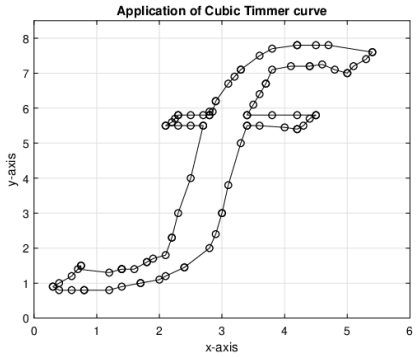

(a) Control polygon

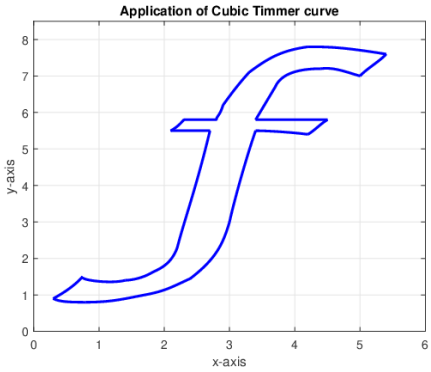

(b) Cubic Timmer Curve

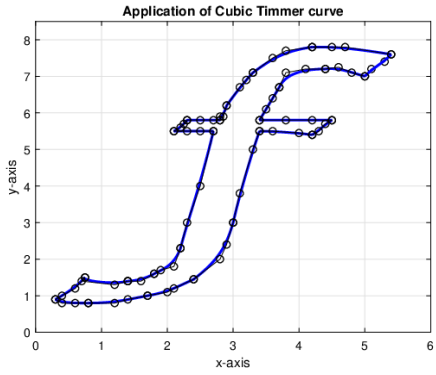

(c) Font together with its control polygon

Figure 5 Letter "f"

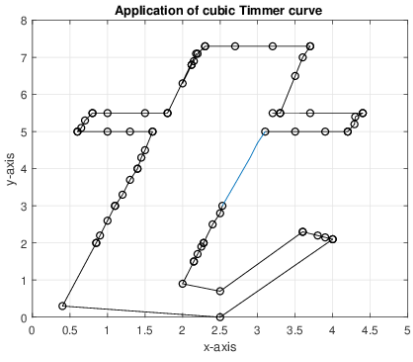

(a) Control polygon

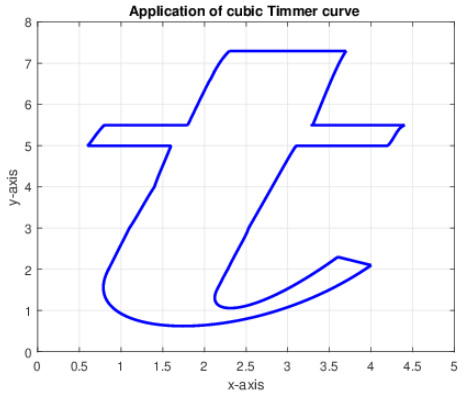

(a) Cubic Timmer Curve

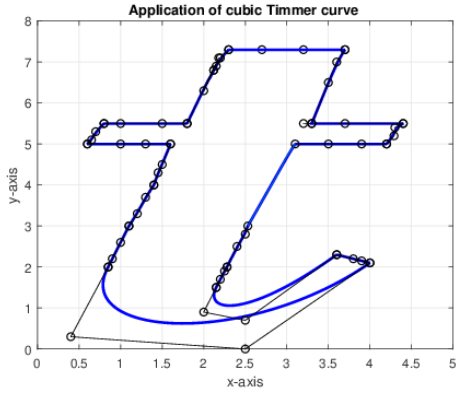

(a) Font together with its control polygon

Figure 6 Letter "t"

2.2 Cubic Triangular Basis Functions

Geometric surfaces usually can be better tiled and constructed with triangles meshes than quadrilaterals meshes because triangular regions can be more natural in partition of the domain [8]. Therefore, arbitrarily shaped surfaces can be constructed. Given three vertices V_1, V_2, V_3 correspond to the barycentric coordinates $(1,0,0), (0,1,0)$ and $(0,0,1)$ respectively. The barycentric coordinates are denote as u, v and w such that any point of the triangle can be written as [6]

$$V = uV_1 + vV_2 + wV_3 , \qquad u + v + w = 1 \qquad (6)$$

A degree n triangular Bèzier patch denoted over a triangular domain is defined as [8].

$$P(u,v,w) = \sum_{i+j+k=n} b_{i,j,k} B^n_{ijk}(u,v,w) \qquad (7)$$

where $b_{i,j,k}$ is the control point of the cubic Bèzier triangular patch that constructed by using de Casteljau algorithm. Meanwhile $B^n_{ijk}(u,v,w)$ is Bernstein polynomials defined by:

$$B^n_{ijk}(u) = \frac{n!\, u^i v^j w^k}{i!\, j!\, k!}, \qquad i + j + k = n, \qquad i,j,k \geq 0 \qquad (8)$$

This equation is called bivariate because one variable is dependent to the other two variables, i.e. $w = 1 - u - v$. The de Casteljau algorithm for a triangular patches is analogous to the algorithm for curves, i.e. repeated linear interpolation [6]. In the cubic form, the control net consists of a few vertices shown in Figure 6;

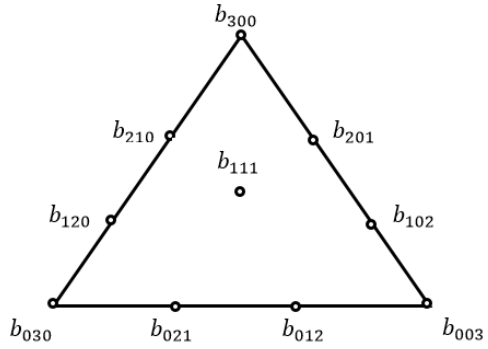

Figure 6 Control net with vertices

The sum of all subscripts in each of the vertices is 3 since it is a cubic case. The control net consists of $\frac{1}{2}(n+1)(n+2)$ vertices. The de Casteljau algorithm can be represented by:

Given: A triangular array of points $b_{i,j,k} \in \mathbb{E}^3; i + j + k = n$ and a point in $\mathbb{E}^2$ with barycentric coordinate u.
Set:

$$b^r_i(\mathrm{u}) = u b^{r-1}_{i,j,k+e1}(\mathrm{u}) + v b^{r-1}_{i,j,k+e2}(\mathrm{u}) + w b^{r-1}_{i,j,k+e3}(\mathrm{u}) \qquad (9)$$

where $r = 1, \ldots, n$ and $i + j + k = n - r$ [7].
Based on the de Casteljau algorithm, the properties of Bèzier triangles are as follows:

a) Affine invariance: Since linear interpolation is an affine map, the de Casteljau algorithm uses the linear interpolation only.
b) Invariance under affine parameter transformations: A point u in the de Casteljau algorithm will have the same barycentric coordinates u after an affine transformation.
c) Convex hull: This property is satisfied since for $0 \leq u, v, w \leq 1$, each of the $b^r_{i,j,k}$ is a convex combination of the previous $b^{r-1}_{i,j,k}$.

2.3 New Cubic Timmer Triangular Patches

The bi-cubic Timmer surface or bivariate cubic Timmer is actually an extension from cubic Timmer curve. It is designed by using tensor product of two or more curves. As mentioned in previous section, the previous method such as cubic Bèzier and Ball triangular patches are formed by using the de Casteljau algorithm. In this study, a new cubic Timmer triangular patch is constructed based on the concept of the previous methods. As a further explanation, Figure 7 shows the control points of cubic Timmer triangular patch and Figure 8 shows the cubic Timmer triangular basis functions.

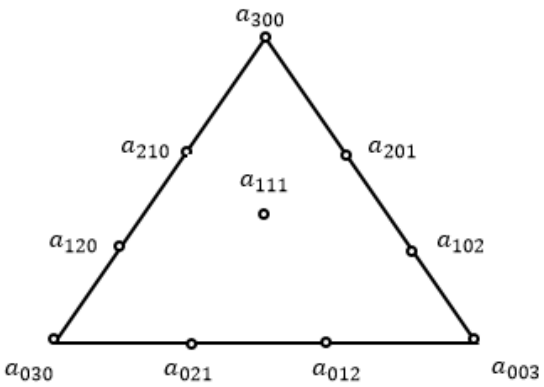

Figure 7 Control points of Timmer triangular patch

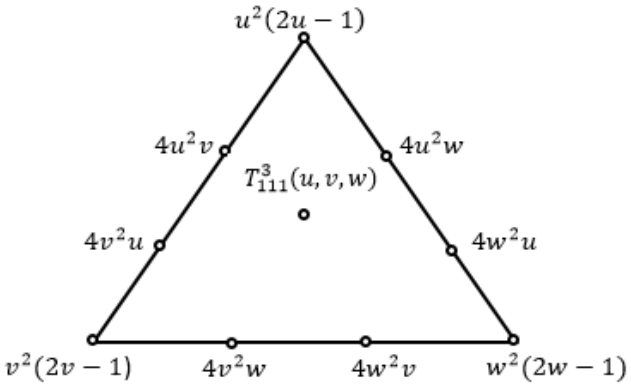

Figure 8 Cubic Timmer basis functions (except inner points)

Based on Goodman and Said [8], the value of each control point for Bèzier and Ball triangular patch is based on the equation of cubic Bèzier and Ball curve. However, for $T^3_{111}(u,v,w)$ which lies in the triangular, is determined by using the property of Bèzier triangular patches which is a partition of unity or mathematically can be denoted as $\sum_{i=0}^{3} B^3_{ijk}(u,v,w) = 1$. As compared to cubic Timmer triangular patch, the value of $T^3_{111}(u,v,w)$ can be obtained by using the same concept as cubic Bèzier triangular patches i.e. by using partition of unity described below:

$$\sum_{i=0}^{3} T^3_{ijk}(u,v,w) = 1$$

$$\begin{aligned} 1 &= u^2(2u-1) + 4u^2v + 4u^2w + \\ &\quad v^2(2v-1) + 4v^2u + 4v^2w \\ &\quad + w^2(2w-1) + 4w^2u + 4w^2v + \\ &\quad T^3_{1,1,1}(u,v,w) \end{aligned}$$

$$\begin{aligned} T^3_{111}(u,v,w) &= 1 - u^2(2u-1) + 4u^2v + 4u^2w + \\ &\quad v^2(2v-1) + 4v^2u + 4v^2w + \\ &\quad w^2(2w-1) + 4w^2u + 4w^2v \end{aligned}$$

When substituting the barycentric coordinates $u+v+w=1$, the value of $T^3_{1,1,1}(u,v,w)$ will be the same as $B^3_{1,1,1}(u,v,w)$ in the cubic Bèzier triangular patch, which fulfilled the partition of unity property.

$$\begin{aligned} T^3_{111}(u,v,w) &= (u+v+w)^3 - \quad u^2(2u-u-v- \\ &\quad w) + 4u^2v + 4u^2w + v^2(2v-u- \\ &\quad v-w) + 4v^2u + 4v^2w + w^2(2w- \\ &\quad u-v-w) + 4w^2u + 4w^2v \end{aligned}$$

$$= 6uvw$$

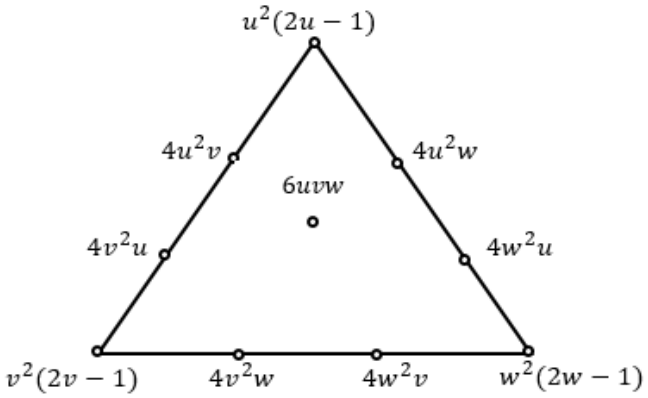

Figure 9 Cubic Timmer basis functions

Figure 9 shows the complete cubic Timmer basis functions. The following theorem is stated the definition of the new cubic Timmer triangular patch:

Theorem 1: A cubic Timmer triangular patch is defined by,

$$T(u,v,w) = \sum_{i+j+k=n} a_{i,j,k} T^3_{ijk} \tag{10}$$

$$\begin{aligned} T(u,v,w) &= u^2(2u-1)a_{3,0,0} + 4u^2va_{2,1,0} + 4u^2wa_{2,0,1} + \\ &\quad v^2(2v-1)a_{0,3,0} + 4v^2ua_{1,2,0} + 4v^2wa_{0,2,1} + w^2(2w- \\ &\quad 1)a_{0,0,3} + 4w^2ua_{1,0,2} + 4w^2va_{0,1,2} + 6uvwa_{1,1,1} \end{aligned} \tag{11}$$

where $a_{r,s,t}$ denoted as the Timmer ordinates of patch T. The derivative of T with respect to the direction $z = (z_1, z_2, z_3) = z_1V_1 + z_2V_2 + z_3V_3, z_1 + z_2 + z_3 = 0$ is given by

$$\frac{\partial T}{\partial z} = \frac{\partial T}{\partial u} z_1 + \frac{\partial T}{\partial v} z_2 + \frac{\partial T}{\partial w} z_3 \tag{12}$$

From (7), it can be shown that

$$\left.\begin{aligned} \frac{\partial T}{\partial u} &= 4v^2 b_{120} + 4w^2 b_{102} + 6vwb^1_{111} \\ \frac{\partial T}{\partial v} &= (6v^2 - 2v) b_{030} + 8vwb_{021} + 4w^2 b_{012} \\ \frac{\partial T}{\partial w} &= (6w_2 - 2w) b_{003} + 4v^2 b_{021} + 8vwb_{012} \end{aligned}\right\} \tag{13}$$

Figure 10 shows some plots of cubic Timmer triangular basis functions.

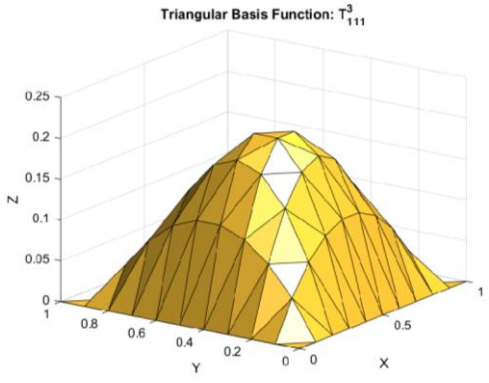

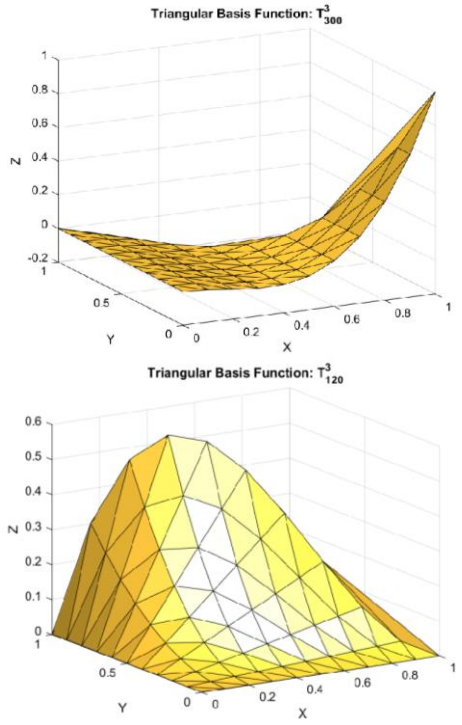

Figure 10 Cubic Timmer triangular basis functions

Theorem 2: *These new Timmer triangular patches have the following properties.*

(a) *Partition of unity*: The property means the sum of the Timmer triangular basis function is 1 or in mathematically can define as below

$$\sum_{i=0}^{3} T_{ijk}^{3}(u,v,w) = 1 \qquad (14)$$

(b) *Symmetry*: The surfaces that formed from two different ordering of its control points will remain the same look.

(c) *Positivity:* Each of the cubic Timmer triangular basis functions is fulfilled the positivity or nonnegativity behavior $T_{ijk}^{3}(u,v,w) \geq 0$, except for certain condition. $T_{300}^{3}(u,v,w) \leq 0$ when $\frac{1}{2} \leq u \leq 1$and both of $T_{201}^{3}(u,v,w) \leq 0$ and $T_{210}^{3}(u,v,w) \leq 0$ when $0 \leq u \leq \frac{1}{2}$. According to the Timmer triangular basis functions stated above, it will not fulfilled the nonnegativity behavior on some interval.

(d) *Convex hull:* The Timmer triangular patches do not all lie within the convex hull of the control polygon. If the positivity property is fulfilled for the Timmer triangular patches so it will ensure the convex hull property.

Figure 11(a) shows the control polygon of the cubic Timmer triangular patch, Figure 11(b) shows the cubic Timmer triangular patch and Figure 11(c) shows the cubic Timmer triangular patch together with its control polygon.

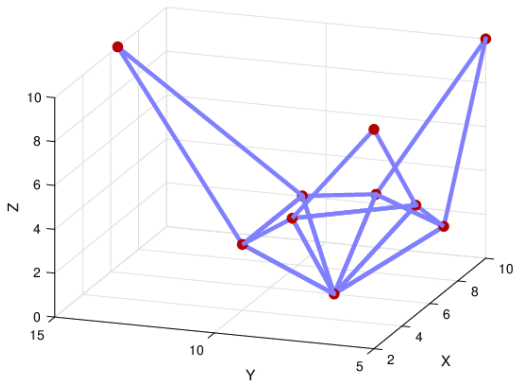

(a) Control polygon

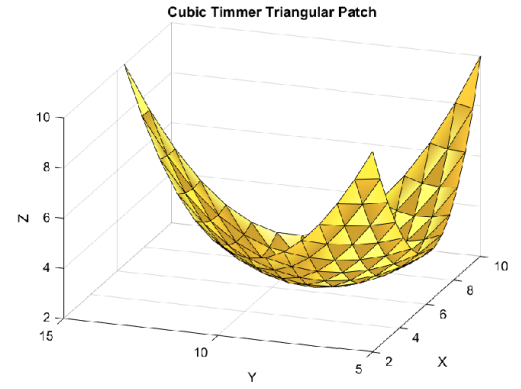

(b) Cubic Timmer triangular patch

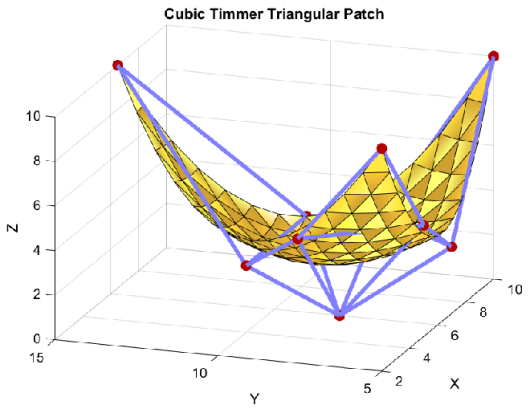

(c) Cubic Timmer triangular patch with its control polygon

Figure 11 Cubic Timmer triangular patch

2.4 C^1 and G^1 Continuity between Adjacent Cubic Timmer Triangular Patches

Let $\Delta U_1U_2U_3$, $\Delta V_1V_2V_3$ be two adjacent triangles on the xy plane with $U_2 = V_3$ and $U_3 = V_2$ in triangle M and N (Figure 12). In this cubic Timmer triangular patches contain Timmer coordinates $b_{i,j,k}$ and $c_{i,j,k}$. These two cubic Timmer triangles have the same boundary curve along the common boundary $U_2 = U_3$, thus $b_{0,3,0} = c_{0,0,3}$, $b_{0,2,1} = c_{0,1,2}, b_{0,1,2} = c_{0,2,1}$ and $b_{0,0,3} =$

$c_{0,3,0}$. The necessary and sufficient conditions for C^1 continuity between the two triangles are

$$c_{1,0,2} = \alpha b_{1,2,0} + \beta b_{0,3,0} + \gamma b_{0,2,1} \quad (15)$$

$$c_{1,1,1} = \alpha b_{1,1,1} + \beta b_{0,2,1} + \gamma b_{0,1,2} \quad (16)$$

$$c_{1,2,0} = \alpha b_{1,0,2} + \beta b_{0,1,2} + \gamma b_{0,0,3} \quad (17)$$

where $V_1 = \alpha U_1 + \beta U_2 + \gamma U_3$, and $\alpha + \beta + \gamma = 1$.

In Farin [4] stated that the concept of geometric continuity is not restricted to curves compared to the parametric continuity. This G^1 conditions is more relaxed because the requirement is not as strict as C^1 conditions to construct the surface.

A G^1 continuity surface on two triangular patches are obtained by obtaining the first order derivatives and the interpolant on each triangle is represented by a single cubic triangular patch. Figure 12 shows an example of Timmer ordinates of adjacent cubic Timmer triangular patches with the common edges $U_2 = V_3$ and $U_3 = V_2$ by triangles M and N respectively where $b_{0,3,0} = c_{0,0,3}$ and $b_{0,0,3} = c_{0,3,0}$ are the vertices ordinates, $b_{1,2,0}, c_{1,2,0}$,$b_{1,0,2}$ and $c_{1,0,2}$ are already obtained from the data points and its gradients while $b_{0,1,2} = c_{0,2,1}, b_{0,2,1} = c_{0,1,2}$, $b_{1,1,1}$ and $c_{1,1,1}$ are the cubic Timmer ordinates to be determined. If the two patches continuously varying tangent plane along the common boundary edge so both patches will satisfy G^1 continuity. The sufficient conditions for G^1 continuity along the common boundary curve and a set of equations can be expressed as follows:

$$U_2 = V_3 \text{ and } U_3 = V_2 \quad (18)$$

$$\alpha b_{1,0,2} + (1-\alpha)c_{1,0,2} = \beta c_{0,0,3} + (1-\beta)c_{0,1,2} \quad (19)$$

$$\alpha b_{1,1,1} + (1-\alpha)c_{1,1,1} = \beta c_{0,1,2} + (1-\beta)c_{0,2,1} \quad (20)$$

$$\alpha b_{1,2,0} + (1-\alpha)c_{1,2,0} = \beta c_{0,2,1} + (1-\beta)c_{0,3,0} \quad (21)$$

where α and β are arbitrary constants. The values of α and β in the equation can be determined using equations of (19) and (20).

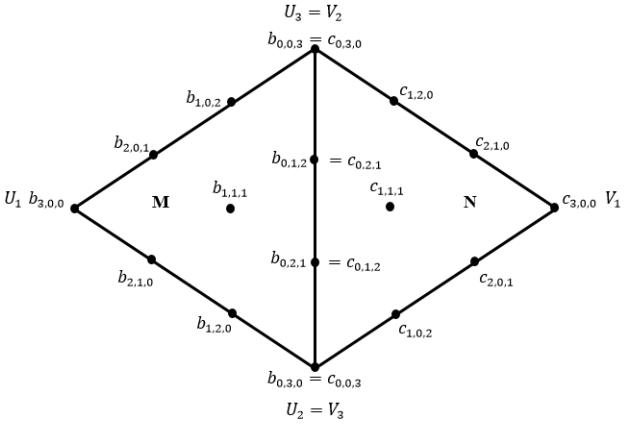

Figure 12 Two adjacent Timmer triangular patches

3.0 RESULTS AND DISCUSSION

The data points are being sampled from the given true function. From Figure 12, there are only three control points need to be calculated from Equations (15) until (17) i.e. $c_{1,0,2}$, $c_{1,1,1}$ and $c_{1,2,0}$.

The main objective, we want to reconstruct the true surfaces but by using two composite triangular patches and comparing the performance against cubic Bèzier triangular patch based on Root mean square error (RMSE) and maximum error (Max). The test functions used are listed below:

1. Franke's exponential function

$$F_1 = \sqrt{\frac{(64 - 81((x-0.5)^2 + (y-0.5)^2)}{9 - 0.5}} \quad (22)$$

2. Steep function

$$F_2(x,y) = \frac{exp\left(-\left(\frac{81}{4}\right)((x-0.5)^2 + (y-0.5)^2)\right)}{3} \quad (23)$$

Table 1 shows the control points that are used in triangle M and N.

Table 1 Control points

x	y	F_1	F_2
Triangle M			
0	1	3.86E-02	1.34E-05
0	0.67	2.15E-01	1.18E-03
0	0.33	2.15E-01	1.18E-03
0	0	3.86E-02	1.34E-05
0.33	0.33	3.56E-01	1.03E-01
0.67	0.67	3.56E-01	1.03E-01
1	1	3.86E-02	1.34E-05
0.67	1	1.79E-01	1.02E-01
0.33	1	1.79E-01	1.02E-01
0.33	0.67	3.56E-01	1.03E-01
Triangle N			
0	0	3.86E-02	1.34E-05
$c_{1,0,2}$			
0.67	0	1.79E-01	1.18E-03
1	1	3.86E-02	1.34E-05
1	0.67	1.79E-01	1.02E-01
$c_{1,2,0}$			
1	0	3.86E-02	1.34E-05
0.67	0.33	3.56E-01	1.03E-01
0.33	0.67	3.56E-01	1.03E-01
$c_{1,1,1}$			

The surface interpolation of cubic Bèzier and cubic Timmer triangular patches for C^1 and G^1 continuity for test function, F_1 illustrates in Figure 13 while for test function, F_2 in Figure 14.

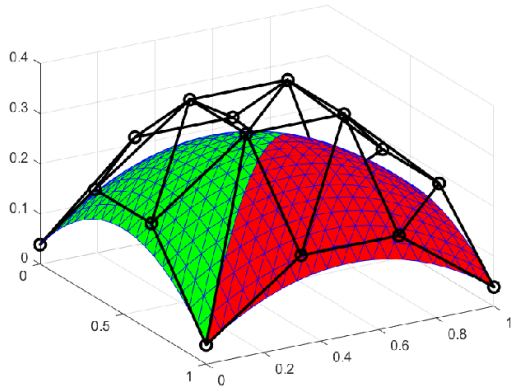

(a) C^1 surface by using cubic Bèzier triangular patches

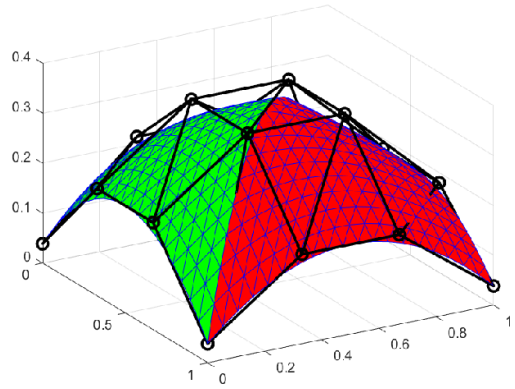

(b) C^1 surface by using cubic Timmer triangular patches

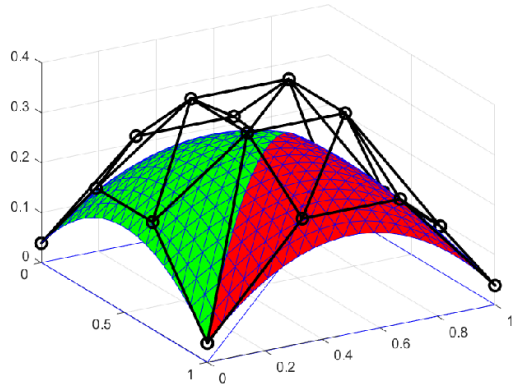

(c) G^1 surface by using cubic Bèzier triangular patches

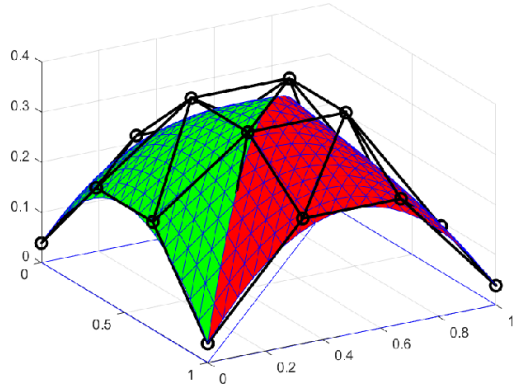

(d) G^1 surface by using cubic Timmer triangular patches

Figure 13 Test Function F_1

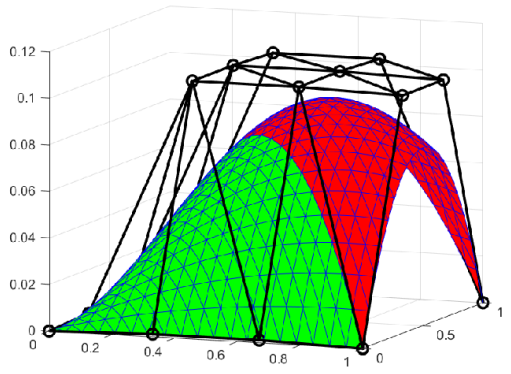

(a) C^1 surface by using cubic Bèzier triangular patches

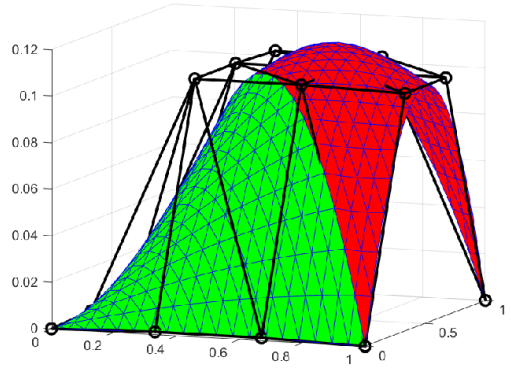

(b) C^1 surface by using cubic Timmer triangular patches

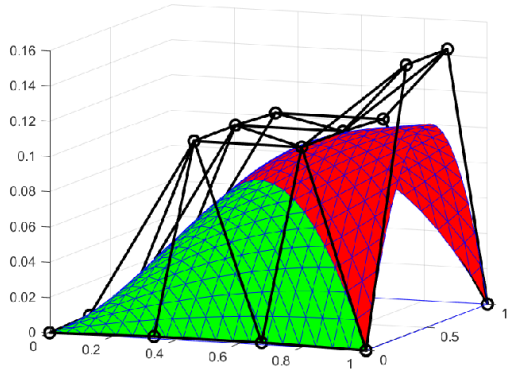

(c) G^1 surface by using cubic Bèzier triangular patches

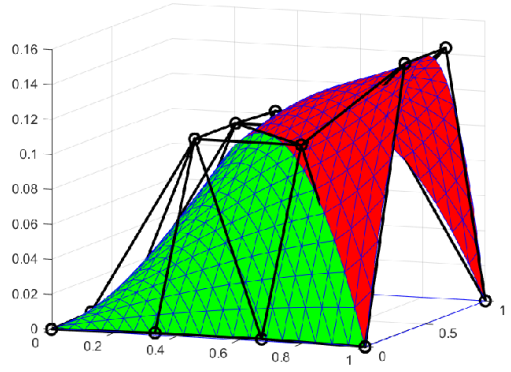

(d) G^1 surface by using cubic Timmer triangular patches

Figure 14 Test Function F_2

Then, the errors for root mean square error (RMSE) and maximum error (Max) is calculated in Table 2. The root mean square error is defined by

$$RMSE = \sqrt{\sum_{i}^{m} \frac{\left(F_i - f(F_i)\right)^2}{m}} \quad (24)$$

where F_i is the value from the scheme, $f(F_i)$ is the test function values and m is the number of the samples.

Table 2 Errors of the test function

Surface	Test Function	Error	RMSE	Max
C_1	F_1	Bèzier	0.0891	0.1157
		Timmer	0.0472	0.0727
	F_2	Bèzier	0.0786	0.2307
		Timmer	0.0710	0.2287
G_1	F_1	Bèzier	0.0929	0.1565
		Timmer	0.0563	0.1434
	F_2	Bèzier	0.0796	0.2347
		Timmer	0.0780	0.2287

Based on Table 2, cubic Timmer triangular patches is the best method since it has less error than cubic Bèzier triangular patches. Then, the values of RMSE and maximum error for cubic Timmer triangular patches formed by using the C^1 continuity less than the G^1 continuity.

4.0 CONCLUSION

In this paper, a new cubic Timmer triangular patch is proposed to construct a better surface. The surface formed by cubic Timmer triangular patches are more approaching to the control polygon compared to cubic Bèzier and Ball triangular patch. This method is based on the concept of Bèzier and Ball method. Then, two patches of cubic Timmer and cubic Bèzier triangular patches that fulfilled C^1 and G^1 continuity are constructed. To compare the effectiveness of these methods, RMSE and maximum error are calculated. Based on the results, cubic Timmer triangular patches are better than cubic Bèzier triangular patches. The surface that fulfilled C^1 continuity is better than G^1 continuity. This new constructed cubic Timmer triangular patch also can be used for surface interpolation in which the data are scattered and non-uniform as discussed in Ali *et al*. [2].

Acknowledgement

This research is fully supported by Universiti Teknologi PETRONAS (UTP) through a research grant YUTP: 0153AA-H24 (Spline Triangulation for Spatial Interpolation of Geophysical Data). The first author is supported by Graduate Research Assistant Scheme (GRA).

References

[1] Ali, J. M. 1994. An Alternative Derivation of Said Basis Functions. *Sains Malaysiana*. 23(3): 42-56.
[2] Ali, F. A. M., Karim, S. A. A., Dass, S. C., Skala, V., Saaban, A., Hasan, M. K., and Ishak, H. 2019. Efficient Visualization of Scattered Energy Distribution Data by Using Cubic Timmer Triangular Patches. To be published by Springer.
[3] Awang, N., and Rahmat, R. W. 2017. Reconstruction of Smooth Surface by Using Cubic Bezier Triangular Patch in GUI. *Malaysian Journal of Industrial Technology*. 2(1).
[4] Awang, N., Rahmat, R. W., Sulaiman, P. S., and Jaafar, A. 2017. Delaunay Triangulation of a Missing Points. *Journal of Advanced Science and Engineering*. 7(1): 58-69.
[5] Brodlie, K., Mashwama, P., & Butt, S. 1995. Visualization of Surface Data to Preserve Positivity and other Simple Constraints. *Computers & Graphics*. 19(4): 585-594.
[6] Chan, E. S., & Ong, B. H. 2001. Range Restricted Scattered Data Interpolation Using Convex Combination of Cubic Bézier Triangles. *Journal of Computational and Applied Mathematics*. 136(1-2): 135-147.
[7] Chang, L. H. T., & Said, H. B. 1997. A C^2 Triangular Patch for the Interpolation of Functional Scattered Data. *Computer-Aided Design*. 29(6): 407-412.
[8] Farin, G. 1986. Triangular Bernstein-bézier Patches. *Computer Aided Geometric Design*. 3(2): 83-127.
[9] Farin, G. 2014. *Curves and Surfaces for Computer-aided Geometric Design: A Practical Guide*. Elsevier.
[10] Foley, T. A., & Opitz, K. 1992. Hybrid Cubic Bézier Triangle Patches. *Mathematical Methods in Computer Aided Geometric Design II*. 275-286.
[11] Goodman, T. N. T., & Said, H. B. 199). A C^1 Triangular Interpolant Suitable for Scattered Data Interpolation. *Communications in Applied Numerical Methods*. *7*(6): 479-485.
[12] Karim, S. A. A., and Saaban, A. 2018. Visualization Terrain Data Using Cubic Ball Triangular Patches. *MATEC Web of Conferences 225*. 06023.
[13] Liu, C. 2001. *Theory and Application of Convex Curves and Surfaces in CAGD*. Faculty of Mathematical Sciences, University of Twente.
[14] Luo, Z., & Peng, X. 2006. A C1-rational Spline in Range Restricted Interpolation of Scattered Data. *Journal of Computational and Applied Mathematics*. 194(2): 255-266.
[15] Mann, S. 2000. Continuity Adjustments to Triangular Bézier Patches that Retain Polynomial Precision. *Polar*. 1(2): 2.
[16] Ramli, N., and Ali, J. M. 2014. Object Design Using Blending of Rational Timmer. *AIP Conference Proceedings*. 1605(1): 262-267.
[17] Ong, B. H., & Wong, H. C. 1996. A C^1 Positivity Preserving Scattered Data Interpolation Scheme. *Series in Approximations and Decompositions*. 8: 259-274.
[18] Saaban, A., Majid, A. A., Piah, M., & Rahni, A. 2009. Visualization of Rainfall Data Distribution Using Quintic Triangular Bézier Patches. *Bulletin of the Malaysian Mathematical Sciences Society*. 32(2).
[19] Said, H. B. 1990. The Bezier Ball Type Cubic Curves and Surfaces. *Sains Malaysia*. 19(4): 85-95.
[20] Said, H. B., & Wirza, R. 1993. *A Cubic Ball Triangular Patch for the Scattered Data Interpolation*. Pusat Pengajian Sains Matematik dan Sains komputer, Universiti Sains Malaysia.
[21] Shepard, D. 1985. A two Diemnsional Interpolation Function for Irregularly Spaced Data. *Proc. ACM Nat. Conf*. 517-524.

[22] Timmer, H. G. 1980. Alternative Representation for Parametric Cubic Curves and Surfaces. *Computer Aided Design.* 12: 25-28.
[23] Wu, J., Zhang, X. and Peng, L. 2010. Positive Approximation and Interpolation Using Compactly Supported Radial Basis Functions. Mathematical Problems in Engineering. Article ID 964528, 10 pages.
[24] Wu, J, Lai, Y. and Zhang, X. 2010. Radial Basis Functions for Shape Preserving Planar Interpolating Curves. *Journal of Information & Computational Science.* 7(7): 1453-1458.
[25] Zhu, Y., Han, X., & Liu, S. 2014. Quartic Rational Said-Ball-like Basis with Tension Shape Parameters and Its Application. *Journal of Applied Mathematics*. Volume 2014, Article ID 857840, 18 pages.